

## State of Art and Future Trends in Photovoltaic Cells and Modules

V. Benda

Czech Technical University in Prague

Received 7 August 2012; Accepted 24 September 2012

### Abstract

After 40 year's development, photovoltaics has been recognized as a renewable energy technology that has the potential to contribute significantly to future energy supply. Material and solar cell and module fabrication technology see to be the most important in the field of photovoltaics, because the progress expectations in photovoltaic applications necessitate a decrease of photovoltaic cell (module) cost on the level of about 30% of today's one. Basic principles of photovoltaic cell physics and technology have been demonstrated on fabrication of crystalline silicon cells and modules, thin film cells and modules, and also new prospective technologies. The aim is to give information important for understanding basic problems of physics, construction and manufacturing photovoltaic cells and modules.

Keywords: photovoltaic module, crystalline silicon cells, thin film modules, fabrication

### 1. Introduction

At the present time, photovoltaics is one of the most dynamically growing industries [1]. Impressive progress in PV technology over the past thirty years is evident from the lowering costs, the rising efficiency and the great improvements in system reliability and yield. Yearly growth rates in the last decade (2000-2011) were on an average higher than 40%, and the global cumulative PV power installed overcame 67 GW<sub>p</sub>. [2] in 2011, as demonstrated in Fig.1.

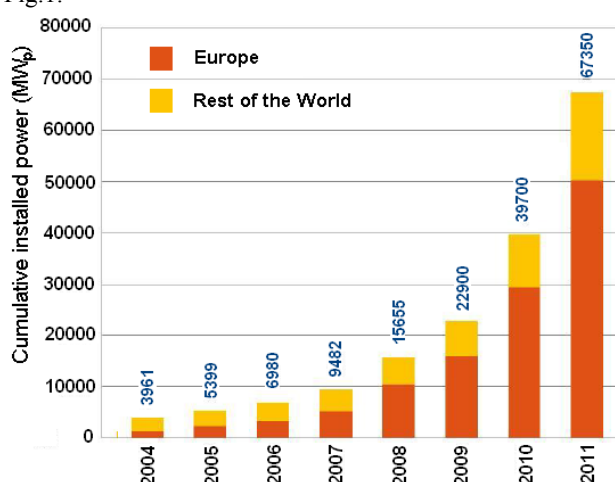


Fig.1. Historical development of World cumulative PV power installed in main geographies

The main fiscal instruments being used to publicly support or promote continue to be the enhanced feed-in

tariffs, with direct capital subsidies also playing an important role. Photovoltaic installations in individual regions in the end of the year 2011 are shown in Fig.2.

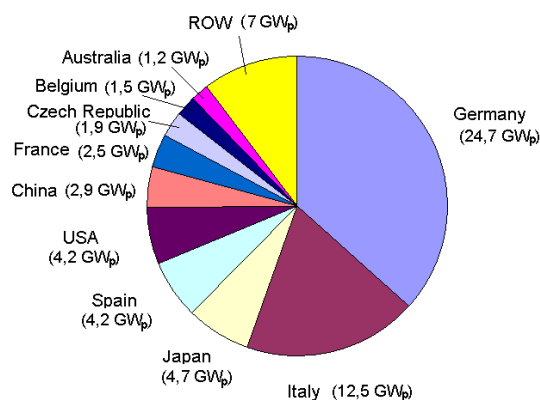


Fig.2. Accumulated PV installations in the World in 2011 (67 GW<sub>p</sub>)

As follows from Fig.1, the most PV installations were realized in Europe, In Europe, the yearly irradiance varies between 800 and 1800 kWh/m<sup>2</sup>. Despite relatively low irradiance level (from 900 to 1300 kWh/m<sup>2</sup>), Germany has become the leading country in photovoltaic installation due to introduction of a feed-in tariff for on-grid systems in 2000. In 1997, the target for cumulative photovoltaic system capacity installed in the European Union by 2010 was stated 3 GW<sub>p</sub>. The real growth rate was much higher than the planned rate, and 3 GW<sub>p</sub> level was reached before the end of 2007. In the EU, the level of 28 GW<sub>p</sub> was reached in 2010 and the level of 50 GW<sub>p</sub> was reached in 2011. In competition with traditional electrical energy sources, photovoltaic systems are fully economical in remote areas, where autonomous PV systems are very important for

\* E-mail address: benda@fel.cvut.cz

spreading information technologies or as local (island) grids. Nevertheless, the most of installed power (over 80%) are on-grid systems, where the energy cost is still higher than in the case of fossil energy sources (standard power plants) and spreading the photovoltaic on-grid power stations has been done mostly by using feed-in tariff. Therefore, the most important task in previous years has been decreasing cost of photovoltaic modules below 1 €/Wp, that means decreasing cost of the PV system below 2 €/Wp with a target to get the PV system cost close to 1 €/Wp [1]. Continuous progress in decreasing the final price of the energy produced from photovoltaic is based on reduction of the production cost of solar cells, keeping the high production yield as well as on enhancing the cell efficiency [3], [4].

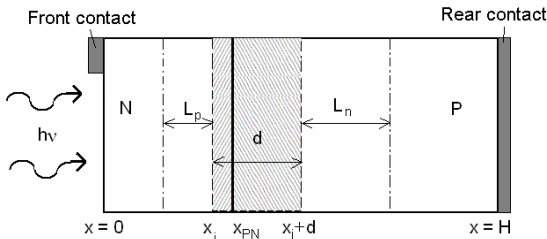


Fig.3. PN junction solar cell structure

**2. Photovoltaic cells and module physics and construction**

Physics and construction of photovoltaic cells and modules have been discussed in details in many publications (e.g. [6], [7], [8], [9], [10], [11], [12]). The structure of a photovoltaic cell can be approximated by a structure shown in Fig.3. In the illuminated area photons with energy higher than band-gap are absorbed generating excess carriers, which diffuse towards the region with built-in electric field (e.g. PN junction or heterojunction) situated in a distance  $x_j$  below the illuminated surface. All generated holes in N-type region reaching the space charge region boundary are drifted by a strong built-in electric field into the P-type region and all electrons generated in P-type region reaching the space charge region are drifted into the N-type region. This way, the P-type region is charged positively, the N-type region is charged negatively, and between both regions is a potential difference. This voltage is capable of driving a current through an external circuit and thereby producing useful work on a load. The density of generated photovoltaic current  $J_{PV}$  consists of carriers generated by incident light with the generation rate  $G$  and collected by the junction space charge region. A part of generated carriers of concentration  $\Delta n$  recombines before reaching the space charge region due to a limited carrier lifetime  $\tau$ . The current density  $J_{PV}$  can be expressed by

$$J_{PV} = q \int_0^H G(x) dx - q \int_0^H \frac{\Delta n}{\tau} dx - J_{sr}(0) - J_{sr}(H) \tag{1}$$

where  $J_{sr}(0)$  represents the surface recombination at  $x = 0$  and  $J_{sr}(H)$  represents the surface recombination at  $x = H$ . The light-induced voltage biases the PN junction in the forward direction. This way, the maximum voltage is limited by the forward I-V characteristic of the PN junction. Then, the solar cell can be modelled as a PV current generator in

parallel with a diode. In a real device, the current of carriers collected by the PN junction flows to output contacts through material with a finite resistance. It means that any solar cell has a series resistance  $R_s$  between the PN junction and output contacts. Imperfections of the PN junction result in a parallel resistance  $R_p$  across the junction. The equivalent circuit of a solar cell is shown in Fig.4.

If  $I$  is the output current,  $V$  is the output voltage and  $R_s$  is the series resistance, across the PN junction is the voltage  $V + IR_s$  forward biasing the diode.

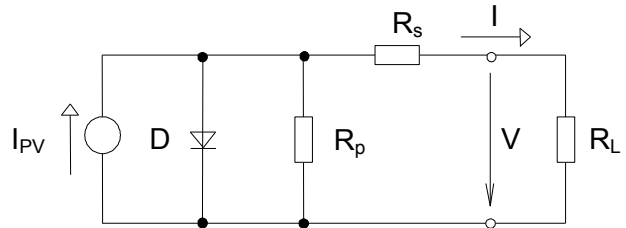


Fig.4. An equivalent circuit of a solar cell

A part of photo-generated current flows through the diode and through the parallel resistance  $R_p$ . Therefore, if  $A$  is the total solar cell area, the output current is given by

$$I = A_{ill} J_{PV} - I_{01} \left[ \exp \left( q \frac{V + R_s I}{\zeta_1 k T} \right) - 1 \right] - I_{02} \left[ \exp \left( q \frac{V + R_s I}{\zeta_2 k T} \right) - 1 \right] - \frac{V + R_s I}{R_p} \tag{2}$$

where  $J_{PV}$  is density of current generated in the volume of the cell structure,  $A_{ill} \leq A$  is the illuminated area of the cell,  $I_{01} = AJ_{01}$  and  $I_{02} = AJ_{02}$ . Important points of I-V characteristic can be derived from (2). The maximum voltage VOC can be obtained from (2) for  $I = 0$ . The short circuit current ISC can be obtained from (2) for  $V = 0$ . For a very low series resistance  $R_s$ , the short circuit current  $ISC \approx A_{ill} J_{PV}$  and it depends very weakly on temperature (a very slight increase). A typical value of JSC for commercial crystalline silicon solar cells is about 35 mA/cm<sup>2</sup> under standard testing conditions (i.e. irradiation 1000 W/cm<sup>2</sup>, spectrum AM1.5, temperature 25°C). ISC decreases with increasing series resistance  $R_s$ . The influence of series resistance  $R_s$  on PV cell efficiency in dependence on irradiance [13] is schematically shown in Fig.6.

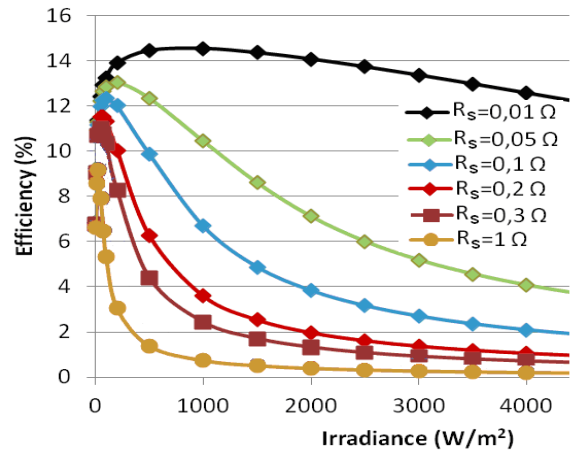


Fig. 6. The influence of series resistance  $R_s$  on PV cell efficiency in dependence on irradiance

Parameters of PV cells depend on temperature. VOC decreases significantly with temperature (for c-Si cells the decrease of VOC is about 0.4%/K), and short circuit current ISC only very slowly increases with temperature. Consequently, the other parameters, maximum power, fill factor and efficiency, also decrease significantly with increasing temperature. In Fig. 7,

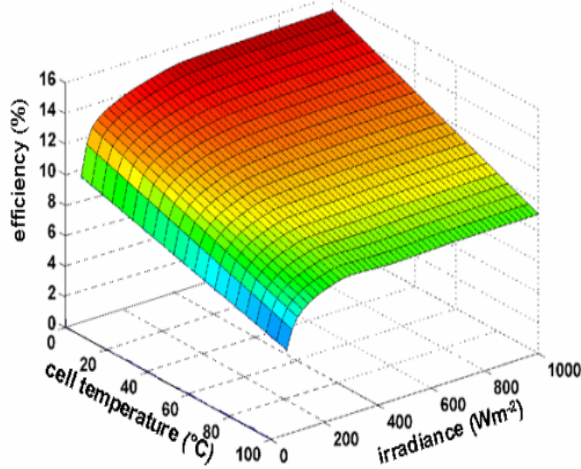


Fig.7. C-Si cell efficiency dependence on temperature and irradiance

an example of the cell efficiency dependence on temperature and irradiance (standard c-Si cell) is shown. From the viewpoint of solar energy conversion in number of generated carriers, this depends strongly on type of semiconductor (band gap, band structure). Photons with too low energy are not absorbed and their energy cannot be transferred in excess carrier generation. Surplus energy of photons with energy higher than band gap is mostly transformed into heat. Then, only a part of incident solar energy can be converted in free charge generation and consequently, in electric power. The maximum efficiency of conversion in dependence on band gap is shown in Fig. 8

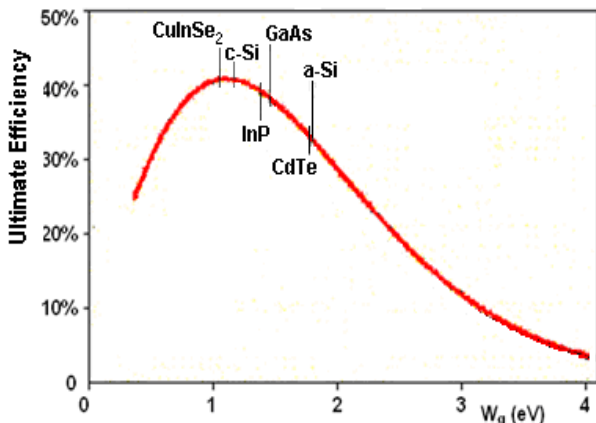


Fig. 8. Maximum conversion efficiency in dependence on bandgap

From that it is possible to evaluate suitability of different semiconductor materials for solar cell fabrication. The photo-generated current density is a difference between carrier generation and recombination in the cell structure. Therefore, the cell construction with respect of individual layer thicknesses strongly depends on the absorption coefficient dependence on photon energy in the solar cell material. Dependences of absorption coefficient on photon energy for different semiconductors are shown in Fig. 9.

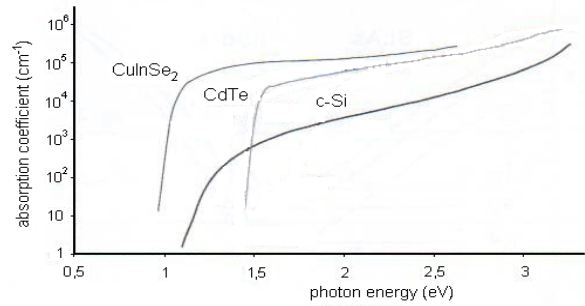


Fig.9. A comparison of absorption coefficients of crystalline silicon, CuInSe<sub>2</sub> and CdTe

Crystalline silicon has relatively low absorption coefficient for wavelength in infrared part of solar spectra. Therefore, a thickness of the base material should be more than 100  $\mu\text{m}$  for an efficient solar cell; and starting material should be a silicon wafer. In some semiconductors, e.g. CdTe or CuInSe<sub>2</sub>, absorption coefficient increases very quickly with photon energy, as shown in Fig. 9. In such material, the whole useable part of solar spectrum is absorbed in a few  $\mu\text{m}$  and the solar cell can be realised in a thin film structure, as indicated in Fig. 10.

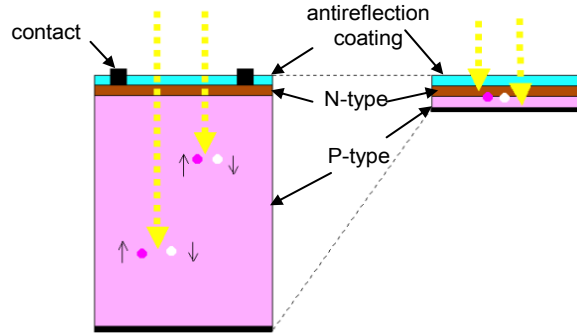


Fig.10. A comparison of wafer base and thin film solar cell construction

Thin film cells can be realised from amorphous silicon (or in combination with microcrystalline silicon), CdTe/CdS, CuInSe<sub>2</sub> (CIS) or CuIn<sub>x</sub>Ga<sub>1-x</sub>Se<sub>2</sub> (CIGS), deposited on a transparent substrate using thin film techniques. Choosing a proper material, the layer thicknesses can be optimised with respect to collecting the possible maximum of carrier generated. On the other hand, in the solar cell structure may be losses, schematically shown in Fig. 11,

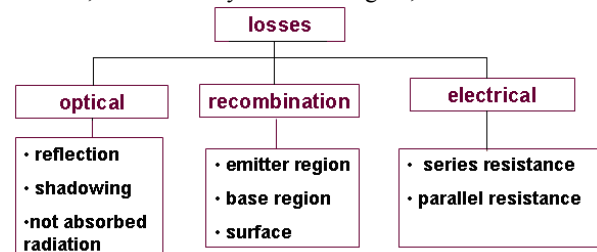


Fig.11. Possible losses in solar cell structures

which must be minimised to obtain high cell efficiency. As the voltage of a single solar cell is low (usually less than 1V), several of them must be connected in series to make a practical generator. A number of cells are usually connected in series and encapsulated in so called modules. The module is the building unit for photovoltaic generator and it is the

real PV product at the market. The I-V characteristics of a PV module can be derived from the scheme in Fig.12.

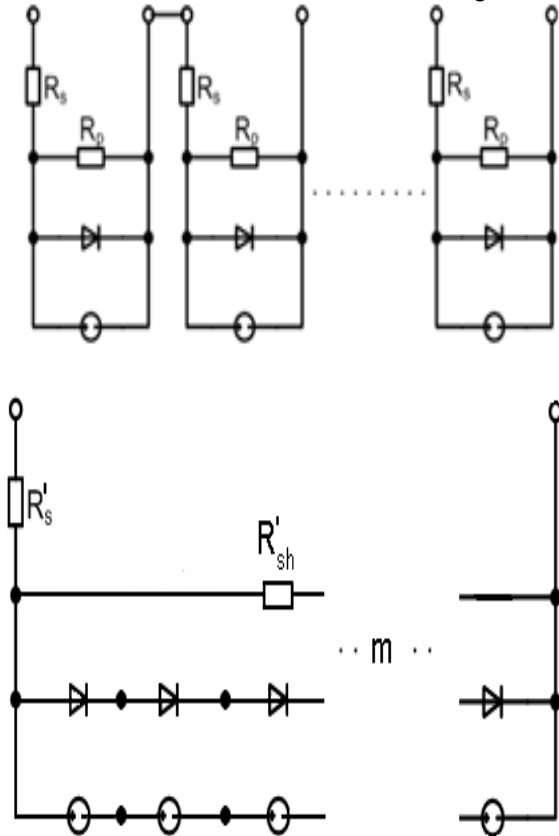


Fig.12. An equivalent circuit of a PV module

Usually, the scheme is simplified using equivalent circuit consisting of a number of current generators in series clamped with the same number of in series connected diodes. Series resistances of in series connected individual cells are replaced with an equivalent module series resistance  $R_s'$  and parallel resistances  $R_p'$ . In this approach, the module I-V characteristic is formally similar to (2). For the module characteristic it is possible to define the same parameters as for photovoltaic cells, i.e. open circuit voltage  $V_{OC}$ , short circuit current  $I_{SC}$ , maximum power  $P_m$ , voltage  $V_{mp}$  and current  $I_{mp}$  in the maximum power point, fill factor  $FF$  and efficiency  $\eta$ . It is very important all in series connected cells have the same  $I_{mp}$  to obtain high module efficiency.

### 3. Crystalline Silicon (wafer based) technology

#### 3.1. Cell Fabrication

Crystalline silicon photovoltaic cells are usually fabricated from P-type Si wafers (monocrystalline or multicrystalline) of thickness in the range of 180-300  $\mu\text{m}$ , prepared from square shaped rods (monocrystalline or multicrystalline) by wire cutting. In the manufacture of (standard) solar cells 6 or more steps are required in succession typically: texturing of the surface, doping, diffusion, removal of the oxide, anti-reflecting coating, metallisation and firing. In the end of the process the cell efficiency and other parameters are measured (under standard testing conditions). Standard cell structure is shown in Fig.13.

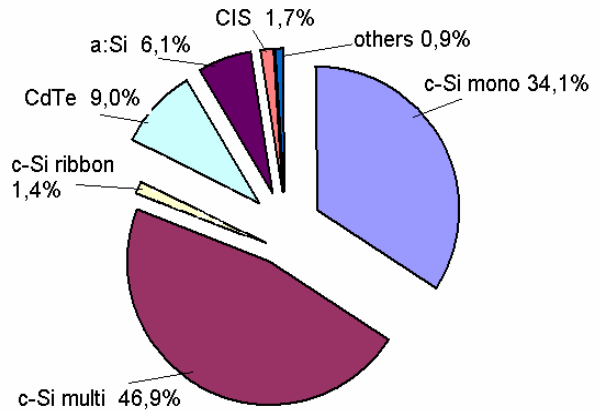


Fig.13. PV Module technology sharing in 2009

Every technological step has a direct or indirect influence on the cell's performance. Some steps influence each other, like diffusion and the material quality (decrease of bulk recombination by gettering), texturing and diffusion (surface cleaning) or the anti-reflecting coating and firing (hydrogen passivation). Standard cell efficiency is about 15-18% for monocrystalline PV cells and 14-17% for multicrystalline PV cells. This design has an efficiency limit of 19% but it has been proved to be ideal in the overall costs. Therefore, more than 85% of PV modules are fabricated now from crystalline silicon, as demonstrated in Fig.14.

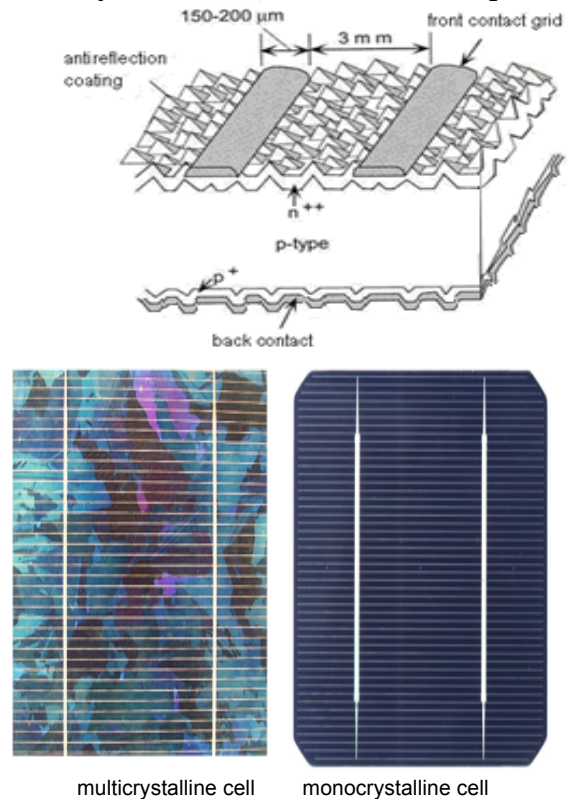


Fig. 14. Standard crystalline silicon cell structure

Improvements in crystalline silicon technology bring a higher starting wafer quality, decrease of both bulk and surface recombination and thinning the wafer result in increase of efficiency and decrease in material consumption, as is demonstrated in Fig.15.

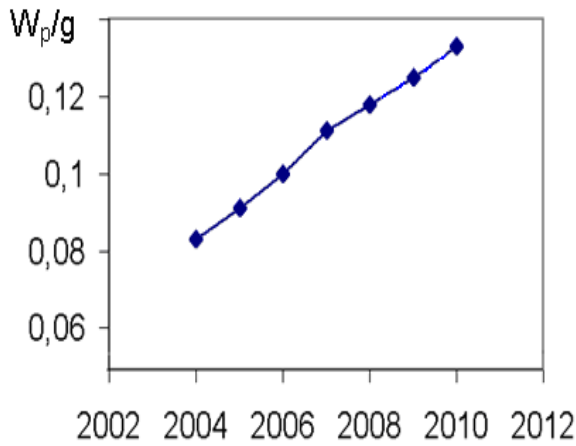


Fig.15. Development of peak power produced from 1 g of crystalline Si

Next improvements in cell efficiency are expected from using N-type starting monocrystalline material [14], using selective emitter decreasing Auger recombination losses [15] and development of all-rear contact technology [16]. Very promising is heterojunction design of HIT cells. Cells on the base of heterojunction between amorphous and N-type crystalline silicon have efficiency over 20% [17]. Some improvements in efficiency need some additional technology steps and resulting cost per Wp is not lower than in the case of standard technology.

### 3.2. Module fabrication

In standard c-Si module technology, tinned copper ribbons (tabs) are soldered to the bus bars at the front to connect the back surface of the next cell, as shown in Fig. 16.

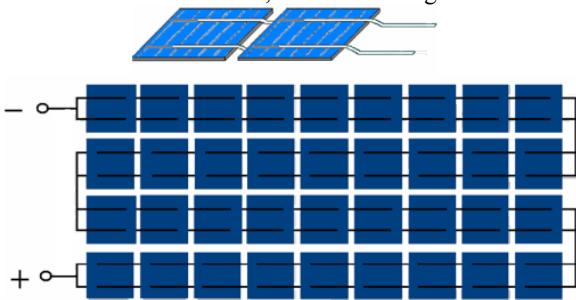


Fig.16. A common module configuration

The tabs must overlap a long distance along bus bar length since the conductance of the printed bus bars is too low. Tabs provide a no rigid link between cells that allow thermal expansions to be accommodated. The strings are interconnected with auxiliary tabs to form the cell matrix, which usually consists of several single strings, as shown in Fig.16. Terminals of the strings are brought outside the module to permit flexible circuit configuration. A 2 to 3 mm thick highly transparent soda lime glass of low iron content is used as a substrate that provides mechanical rigidity and protection to the module while allowing light through. The cell matrix is sandwiched between two layers of the transparent encapsulant material. The most popular encapsulant is the copolymer ethylene-vinyl-acetate (EVA). At the non-illuminated module side is usually used as the outer layer a composite plastic (tedlar) sheet or another glass acting as a barrier for humidity and corroding species. The next fabrication steps are lamination and curing. The standard module structure is demonstrated in Fig.17.

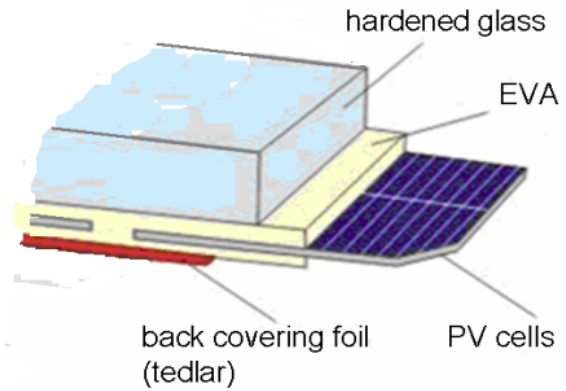


Fig.17. Structure of a standard crystalline silicon PV module

To eliminate possible hot spot origin, the approach followed is to put a diode (bypass diode) in parallel, but in opposite polarity, with a group of cells. This is an important protection of modules against e.g. local shading. The most important components of c-Si module fabrication cost are shown in Fig. 18.

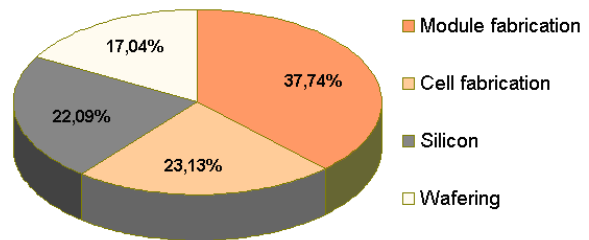


Fig.18. Cost structure of crystalline silicon PV

Continuous technological development brings significant decrease of cost both of silicon and wafering and also some other technological operations in the crystalline silicon cell technology.

## 4. Thin film solar cell and module technology

Thin film cell construction needs a substrate on which it is realised. The substrate can be either metallic or a transparent insulator (glass or plastic). Very thin layers of the cell structure have relatively high sheet resistance and to avoid high electrical losses it is necessary optimise the current flow over resistive path in the front layer of the cell. To solve this problem, electrical contacts on the front surface of cells are realised by a layer of transparent conducting oxide (TCO). Suitable TCO materials are tin oxide SnO<sub>2</sub> doped with fluorine, In<sub>2</sub>O<sub>3</sub> doped with 9% of Sn (so called ITO – indium tin oxide) and zinc oxide ZnO doped with aluminium. Basic technologies that can be used for thin film cell fabrication are vacuum deposition and CVD (Chemical Vapour Deposition). The most important materials for thin film cells are amorphous silicon and CdTe, prospective is also Cu(InGa)Se<sub>2</sub>.

### 4.1. Amorphous silicon thin film cells

Amorphous Si is deposited from hydride gases such as SiH<sub>4</sub> using plasma to decompose the gas. This is called plasma-enhanced CVD (PECVD) and allows for large areas to be coated rather uniformly and with excellent control by temperature and gas composition. The material has 1 to 10% hydrogen bonded to the Si, and is often designated as a-Si:H. The H atoms passivate a large number of the defects

resulting from the incomplete bonding of the Si atoms. The atomic structure has no long-range order like all other crystalline or polycrystalline materials. This can be an advantage. Films are typically deposited between 150 to 300°C. The low deposition temperature allows using lower-cost, low-temperature substrates (glass, stainless steel foil, or plastic). The PIN structure is formed by doping the thin contact layers as they grow with doping gases containing the boron or phosphorous atoms, as shown in Fig.19 a.

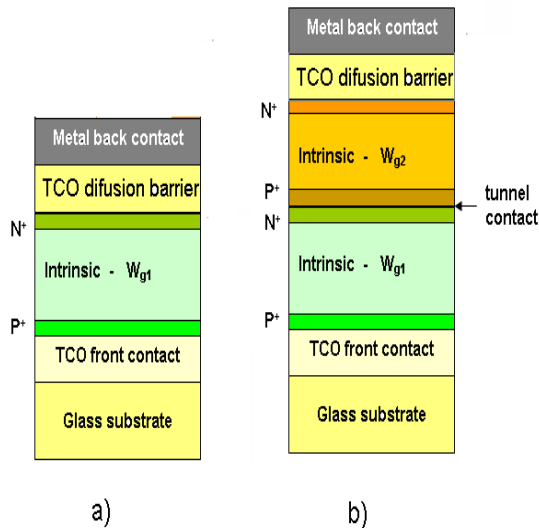


**Fig.19.** Structure of thin film cells on the base of amorphous silicon on transparent substrate  
 a) simple a-Si cell  
 b) two material multiple junction structure

Many types of a-Si modules contain multiple junction devices where two or three junctions are grown on top of each other, as shown in Fig.19 b. The light is coming through the transparent substrate (glass) and TCO front contact in the first cell with material with  $W_{g1}$ , (usually amorphous silicon) where is absorbed a part of spectrum (shorter wavelengths). The part of non absorbed light penetrates into the second cell of material with  $W_{g2}$  ( $W_{g2} < W_{g1}$ ), where is absorbed. As the second material is used a-SiGe, or microcrystalline silicon. The in series connected PIN cells are connected with a tunnel P+N+ junction. The multiple junction cells may be realized in situ by changing reaction gas composition. It is very important all in series connected cells have not too different  $I_{mp}$  to obtain high module efficiency. The efficiency of multiple junction thin film cells in mass production is about 10%. The advantage of amorphous silicon thin film cells is that their efficiency is much less temperature dependent in comparison with crystalline silicon, in supply-chain and reduced capital cost. If the substrates are flexible (stainless steel or plastics), “roll-to-roll” manufacturing where all the layers are deposited as the roll moves through their process zone can be used [10].

#### 4.2. CdTe thin film cells

Polycrystalline layers of CdTe have been investigated for photovoltaics since the 1970s. The commonly used structure based on heterojunction between CdS and CdTe is shown in Fig.20.

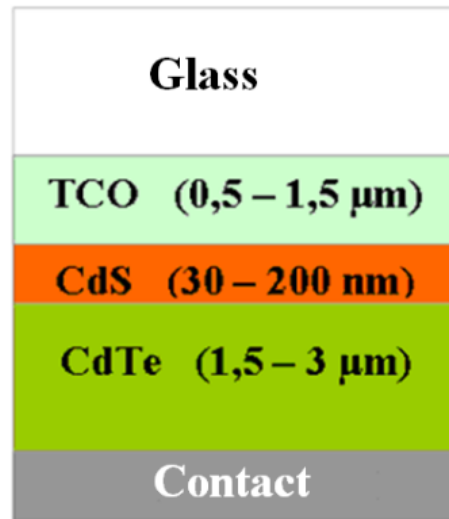


**Fig. 20.** Structure of CdTe thin film cell

The heterojunction is formed by first depositing an n-type layer of CdS on a transparent conductive oxide substrate followed by deposition of CdTe layer and appropriate chemical annealing. There are over 10 methods to deposit the CdTe have produced PV cells exceeding 10% efficiency [10], mostly is used close spaced sublimation method (CSS). Using CSS method, CdTe heated in vacuum up to above 600°C sublimates and CdTe films condense on substrate (glass covered with TCO and CdS layers) kept on temperature 450-600°C (below soften glass point). CdTe deposition rates of  $\mu\text{m}/\text{min}$  can be achieved. The CdTe films are slightly p-type, typically, 2 to 8  $\mu\text{m}$  thick and have crystallites or grains on the order of 1  $\mu\text{m}$ . After CdTe layer deposition, a post-deposition anneal in the presence of Cl and  $\text{O}_2$  at around 400°C is necessary. This chemical/thermal treatment enlarges the grains, passivates the grain boundaries, and improves the electronic quality of the CdTe. Before applying a rear contact, CdTe layers need a surface treatment by etching away unwanted oxides and leaving a Te-rich layer needed to make a low-resistance contact that needs a Cu-containing material somewhere in their CdTe contact process. An advantage of CdTe PV cells is a lower temperature dependence of efficiency in comparison with crystalline silicon cells and relatively low cost of technology process. On the other hand, tellur is relatively rare (and expensive) material that is a disadvantage and it is not expected CdTe can take over bulk silicon market [25].

#### 4.3. Thin film module technology

There is possible to use structuring individual layers by laser cutting and preparing a module consisting for several in series connected solar cells on one glass substrate, as shown in Fig. 21.

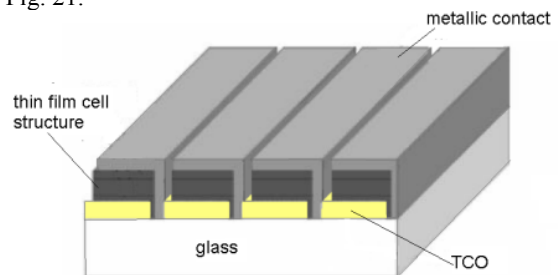


**Fig.21.** A thin film module construction

In this case, the sequence of technological operations is following:

- cleaning glass substrate
- TCO deposition using CVD or sputtering technique and texturing
- TCO layer is “scribed” by a laser into strips about 10-20 mm wide
- deposition of the thin film PV cell structure
- another laser scribing is done at this point adjacent to the first scribe lines. This second scribing is done at a lower laser power so that, thin film PV cell layers are scribed, the underlying TCO layer remains intact
- a metal layer (usually aluminium) is sputter-deposited as the back reflector and back contact.
- the third scribing of the metal contact adjacent to the second completes the inter-connection of neighbouring cells in series (the module structure after this is shown in Fig.21)
- the fourth, high-power laser scribing around the perimeter of the module isolates the active area from the edges
- outline leads are connected using highly conducting adhesives [22]
- the module is then encapsulated by bonding a second glass plate or a tedlar foil onto the cells with EVA.

### 5. Discussion

Growing demand for photovoltaic applications significantly increased demand for solar grade silicon and after 2005 there was a shortage of starting silicon material. That time were prepared many investments in thin film technologies that start to cover more significant part of the market. From 2008 to 2010, solar-grade silicon production more than tripled [18] from approx. 37,000 MT to approx. 121,000 MT. After resolving the poly silicon bottleneck in 2009, new projects for new wafer based manufacturing sites started to grow significantly and also the cost of crystalline silicon modules decreased significantly. Wafer based technology represents approximately 88% of today’s market share, whereas thin film based technologies represent the remaining 12%. The cost level in 2011 is shown in Fig. 22.



Fig.22. PV module cost in the year 2011

In 2009, the cost of PV modules represented about 55% of the total cost of the system. Since then, the cost of modules has decreased significantly while the cost of BOS slightly increased, so at present the cost of PV modules represents about 45% of the total PV system cost. It gives further advantage crystalline silicon modules of higher efficiency that need less BOS portion in the system cost. A comparison of the cost structure in 2009 and 2011 is done in Fig. 23.

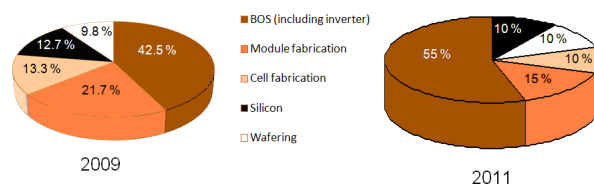


Fig.23. Comparison of the cost structure of PV systems from crystalline silicon modules in 2009 and 2011

The cost of thin film modules should be significantly lower than that of c-Si ones. From present development follows, that all discussed technologies already reached a cost level below 1 €/Wp. A roadmap for decreasing cost of crystalline silicon PV modules below 0.5 €/Wp has been discussed in [5]. Very important is also durability of PV modules. At present, durability of minimum 20 years is expected for all technologies on the market, but the efficiency decrease of c-Si modules in PV power stations built in 80’s was about 0.5% a year. This gives durability higher than 30 years. If typical durability is increased from 20 to 30 years, the cost per generated kWh is reduced by 30%. Grid parity could be achieved even now in many countries by this alone. Besides the main technology streams, intensive research and development is done in other very promising new emerging technologies like Dye-sensitised cells, organic cells, quantum dots PV cells and concentrator cells. All these technologies should reach both cost and durability levels of present technologies [24] to find its place on the market.

### 6. Conclusion

The production processes in the solar industry still have great potential for optimisation both wafer based and thin film technologies. The PV module cost is at present below 1 €/Wp and a decrease of a residential PV system cost on a level of 1,5 €/Wp before 2015 can be expected. In future, further progress can be achieved by new processes, new tools based on this processes, new materials and new designs of products.

### References

1. Jäger-Waldau, A., *PV Status Report 2011*, EUR 24807 EN, 2011
2. <http://files.epia.org/files/Global-Market-Outlook-2016.pdf> (May 2012)
3. EC Communication {SEC(2009) 1257}
4. Breyer, 24th EU PVSEC, Hamburg, (2009)
5. Fischer, M., et al, International Technology Roadmap for Photovoltaics (ITRPV.net) Results 2010, March 2011

6. Fonash S.J., „Solar Cell Device Physics“, Academic Press, 1981.
7. Wagemann, H.G. and Eschrich, „Grundlagen der photovoltaischen Energiewandlung“, Stuttgart, Teubner, 1994
8. Goetzberger A., Knobloch J., Bernhard V., „Crystalline Silicon Solar Cells“, John Wiley & Sons, Inc., 1998.
9. Photovoltaic and Photoactive Materials – Properties, Technology and Applications (edited by J.M. Marshall and D. Dimova-Malinovska), NATO Science Series, Kluwer Academic Publishers, 2002
10. Handbook of Photovoltaic Science and Engineering (edited by A. Luque and S. Hegedus), J. Wiley & Sons, 2003
11. Würfel, P., „Physics of Solar Cells“, Wiley-VCH Verlag, Weinheim, 2005
12. Markvart, T. and Castaner, L., Solar Cells – Materials, Manufacture and Operation, Elsevier, 2005
13. Benda, V. - Macháček, Z., *Proceeding MedPower 2010*
14. A. R. Burgers et al.: 25th European Photovoltaic Solar Energy Conference, 2010, Valencia
15. G. Hahn, 25th European Photovoltaic Solar Energy Conference, 2010, Valencia
16. F.Clement, 25th European Photovoltaic Solar Energy Conference, 2010, Valencia
17. H. Sakata et al., 25th European Photovoltaic Solar Energy Conference, 2010, Valencia
18. H. A. Aulich, F.-W. Schulze, O. Anspach: 25th European Photovoltaic Solar Energy Conference, September 2010, Valencia
19. H. W. Schock: 25th European Photovoltaic Solar Energy Conference 6-10 September 2010, Valencia
20. B. Dimler, 21th European Photovoltaic Solar Energy Conference, 2006, Dresden
21. C. del Canizo, G. del Coso and W.C. Sinke, Prog.Photovolt: Res. Appl. 2009, 199-209
22. R Wells and M. Francis, 25th European Photovoltaic Solar Energy Conference, 2010, Valencia,
23. S. Leu, A. Richter , 25th European Photovoltaic Solar Energy Conference, 2010, Valencia,
24. D. Sera, *Real-time Modelling, Diagnostics and Optimised MPPT for Residential PV systems*, Thesis, Aalborg University, 2009
25. R. Singh, G.F. Alapatt, and K.F. Poole, Proc. 28th International Conference on Microelectronics (MIEL 2012), Nis Serbia, 2012, 53-63